DOI: https://doi.org/10.33103/uot.ijccce.22.2.2

PAPR Reduction for Different O-OFDM in VLC Using μ-Law Companding and Convolutional Encoder

Samir M. Hameed[1], Sinan M. Abdulsatar[2], Atheer A. Sabri[3]

[1]*University of Information Technology and Communications, Baghdad, Iraq*

[2]*Electrical Engineering Department, University of Technology, Baghdad, Iraq*

[3]*Communication Engineering Department, University of Technology, Baghdad, Iraq*

[1]*samirmhameed@uoitc.edu.iq*, [2]*sinan.m.abdulsatar@uotechnology.edu.iq*, [3]*atheer.a.sabri@uotechnology.edu.iq*

Abstract— *Researchers have extensively utilized optical orthogonal frequency division multiplexing (O-OFDM) in visible light communication (VLC) to achieve high data rate transmission for free spectrum bandwidth. The peak-to-average power ratio (PAPR) is the critical challenge for VLC systems-based O-OFDM that produces non-linearity and degrades performance. In this paper, a proposed model for PAPR reduction can be applied with different O-OFDM technologies. This model considered using μ-law companding with O-OFDM transmitter to compress high amplitude peaks and restore the signals using de-companding in the receiver. The obtained simulation results show an efficient achievement of about 75% PAPR reduction compared with the original O-OFDM for different techniques. Furthermore, The convolutional encoder with Viterbi decoder is used with our proposed model for improvement BER performance and tradeoff with PAPR. The BER performance for different coding schemes, O-OFDM technologies, and modulation orders has been graphed and compared. It can notice the convolutional encoder/Viterbi satisfies better BER than Hamming coding/decoding. However, the number of memory cells of the convolutional encoder plays an essential role in BER improvement.*

Index Terms— *ACO-OFDM, ADO-OFDM, DCO-OFDM, PAPR, VLC.*

I. INTRODUCTION

Recent interest in visible light communication (VLC) has grown due to its ability for high data rates communications and overcoming the issue of spectrum congestion compared to wireless radio communications [1]–[5]. VLC can be used in many applications such as indoor wireless communications, intelligent transportation systems, smart cities, warehouses/robotic localization, the entertainment industry, and hospitals [6]. Light-emitting diodes (LEDs) transmit the information as intensity, and photodiodes (PDs) are used as receivers in VLC systems. The Optical orthogonal frequency division multiplexing (O-OFDM) is a promising modulation technology for VLC due to its immunity to inter-symbol interference at higher data rates [7]. In contrast to classical OFDM, O-OFDM is explicitly adopted with the intensity modulation/direct detection (IM/DD) technique to use non-negative, non-complex symbols instead of bipolar complex signals [8]. O-OFDM for IM/DD has been proposed in many different schemes depending on the methods for converting bipolar to unipolar symbols: DC biased O-OFDM (DCO-OFDM) [9], Asymmetrically clipped O-OFDM (ACO-OFDM) [8], flip-OFDM [10], and asymmetrically clipped DC biased O-OFDM (ADO-OFDM) [11]. The nonlinearity of LED and the peak-to-average power ratio (PAPR) are the main challenges in VLC and OFDM systems that reduce VLC performance. In [9], the performance of VLC based O-OFDM with different non-linearity degrees was studied. The pre-distortion adaptive estimation method was

Received 27/August/2021; Accepted 18/October/2021

 ISSN (Print) 1811-9212 *ISSN (Online) 2617-3352*

DOI: https://doi.org/10.33103/uot.ijccce.22.2.2

used to compensate LED non-linearity [12]. Our recent works [11], [13] have studied the VLC performance; in [2], the enhanced ADO-OFDM was proposed with Hamming coding/decoding to improve performance, and in [13], precoding techniques with Viterbi decoding was utilized with different O-OFDM to alleviate LED non-linearity. There are many methods were exist to overcome the PAPR problems in O-OFDM systems; these methods were proposed to reduce PAPR, such as the clipping method [14], partial transmit sequences (PTS) [15], selective mapping (SLM) [16], and non-linear companding techniques [7]. The shortcomings of PAPR reduction methods such as the complexity, bit-error-rate (BER) degradation, and the average optical power swelling make the non-linear companding method is the best option for the PAPR issue. There are different companding functions such as logarithmic, hyperbolic tangent, A-law, and μ-law [7], [17]. The μ-law function has been given the finest companding [17]–[19]. In this paper, ACO-OFDM, ADO-OFDM and DCO-OFDM are presented to use in VLC. However, the PAPR issue is illustrated and compared for different O-OFDM. PAPR mitigation method is proposed to use a convolutional encoder and μ-law compander with an O-OFDM transmitter. The proposed compander is used to weaken the higher peaks and strengthen the weak peaks. In the receiver, the de-companding and Vetribi decoder are employed with the O-OFDM receiver. The de-companding process is the compander's reverse function, which restores the O-OFDM signal to its original form. Consequently, the Viterbi decoder rule is to improve BER and alleviate the non-linearity. The proposed model is compared with other companding methods such as clipping method and combination model of μ-law and clipping. The proposed model combines the benefits of μ-law companding, which lowers PAPR and the Vetribi decoder that improves BER. Three encoder methods are utilized to analyze the BER and compare them to find the optimum improvement.

The rest of the paper structure is as follows: Section II presents the system model. The proposed model is discussed in section III. Section IV shows the simulation results and discussion. Section V concludes the paper.

II. SYSTEM MODEL

In VLC systems, the intensity of LED is modulated by O-OFDM. The optical wireless communication system performance is enhanced by using a multicarrier modulation scheme that ensures orthogonality by O-OFDM [20]. The O-OFDM symbols must be non-complex and non-negative to be suitable for IM/DD process. In this section, the concepts of DCO-OFDM, ACO-OFDM, and ADO-OFDM are explained. The mathematical model is detailed, and the PAPR issue is illustrated

A. DCO-OFDM

Generally, the O-OFDM uses an IFFT block diagram to convert the frequency domain of the overlapping subcarriers to the time domain [9]. The Hermitian symmetry is employed in O-OFDM techniques to transform complex signals into real values [8]. *Fig. 1* shows the block diagram for DCO-OFDM; the source signals are mapped into complex symbols by the M-QAM modulator, and the symbols are framed after converting from serial-to-parallel (S/P), then Hermitian symmetry is applied as follows [8]:

$$X_{N-k} = X_k^{*} \quad , for\ k=0\ to\ N/2 \tag{1}$$

where $X_0=X_{n/2}=0$, N is the total number of subcarriers frequencies, and X_k is the mapping data in the frequency domain. The general IFFT equation can be written as [21]:

Received 27/August/2021; Accepted 18/October/2021
 ISSN (Print) 1811-9212 ISSN (Online) 2617-3352

DOI: https://doi.org/10.33103/uot.ijccce.22.2.2

$$X_n = \frac{1}{\sqrt{N}} \sum_{k=0}^{N-1} X_k e^{\frac{i2\pi nk}{N}} \quad for\ 0 \leq n \leq N\text{-}1 \tag{2}$$

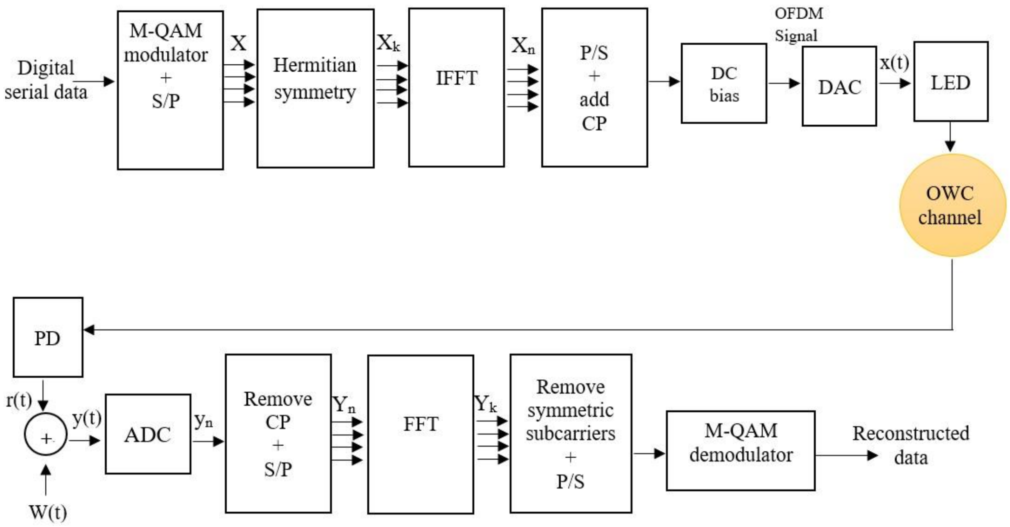

FIG. 1. DCO-OFDM BLOCK DIAGRAM.

After IFFT, the O-OFDM symbols did not include any symbol with a complex number, and each symbol carries sets of mapping symbols. In DCO-OFDM, the actual data is transmitted by half of the subcarriers used in the classical O-OFDM due to Hermitian symmetry [11]. The DC bias is added to DCO-OFDM symbols to pull up and obtain non-negative symbols for IM/DD scheme. The DC bias value will characterize the PAPR and average optical power [21]. The Cyclic prefix (CP) extension is added to O-OFDM symbols to avoid intersymbol interference and is chosen concerning coherence time [20]. The O-OFDM signals are converted to analog signals using a digital-to-analog converter (ADC) for intensity modulation. The PD at the receiver side detects the intensity indicated by the transmitter LEDs. The received signal is y(t) can be written as [16]:

$$y(t) = r(t) + W(t) \tag{3}$$

where W(t) is additive white Gaussian noise (AWGN) includes shot noise and thermal noise, and r(t) can be written as:

$$r(t) = x(t) * h(t) \tag{4}$$

where x(t) is the transmitted O-OFDM signals, * is the convolution process, and h(t) is the optical wireless communication (OWC) channel impulse response. The OWC can be categorized as line-of-sight (LOS) or non-line-of-sight (NLOS) channels. In the NLOS case, the equalizer and channel estimator is added to the O-OFDM receiver for compensation for the multipath effects [13]. Then the CP extensions are removed, and the demodulation process is accomplished after the FFT process, which retrains the signals in the frequency domain.

Received 27/August/2021; Accepted 18/October/2021

DOI: https://doi.org/10.33103/uot.ijccce.22.2.2

B. ACO-OFDM

ACO-OFDM technique had been proposed to reduce the dependence on DC bias [8]. However, the actual data is sent only by the odd subcarriers in ACO-OFDM, so the spectral efficiency of the VLC is reduced to half of the DCO-OFDM [11].

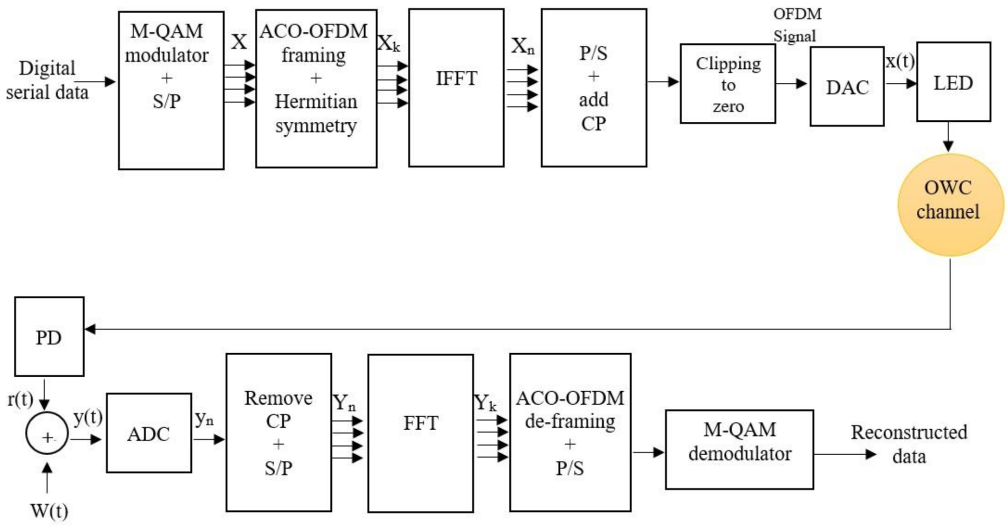

FIG. 2. ACO-OFDM BLOCK DIAGRAM.

Fig. 2 presents the ACO-OFDM block diagram, similar to the DCO-OFDM, but generating non-negative O-OFDM symbols is different at the transmitter. The ACO-OFDM framing is done by assignment data only for odd subcarriers and leaving the even components. So, the input signal to IFFT in ACO-OFDM can be written as follows [20]:

$$X_k = [0 \;\; X_1 \;\; 0 \;\; X_3 .... X_{N/2}] \tag{5}$$

After applying Hermitian symmetry and adding CP extensions, the clipping to zero is used to produce ACO-OFM for IM/DD process. All negative values are removed after the clipping process without losing information due to symmetry [20]. At the ACO-OFDM receiver, the signal is converted to an electrical domain by PD. It is converted to a digital signal for processing via an analog-to-digital converter (ADC); the FFT process is applied by using general formula as follows [13]:

$$Y_k = \frac{1}{\sqrt{N}} \sum_{n=0}^{N-1} Y_n e^{\frac{-i2\pi nk}{N}} \quad for\ 0 \leq k \leq N\text{-}1 \tag{6}$$

where Y_k is the received signal frequency domain, the demodulation process is done by extracting the odd components for M-QAM demodulation and reconstructing the data.

C. ADO-OFDM

The power efficiency of DCO-OFDM is influenced by DC bias and the low spectral efficiency in ACO-OFDM, which prompted ADO-OFDM development [8], [11], [20], [21]. ADO-OFDM is a hybrid model consisting of ACO-OFDM and DCO-OFDM [8]. The odd subcarriers are used to transmit data based on ACO-OFDM, while the DCO-OFDM uses the even subcarrier [11], [21]. The generated ADO-OFDM is given by [11]:

Received 27/August/2021; Accepted 18/October/2021

ISSN (Print) 1811-9212 ISSN (Online) 2617-3352

DOI: https://doi.org/10.33103/uot.ijccce.22.2.2

$$X_{ADO} = X_{ACO} + X_{DCO} \quad (7)$$

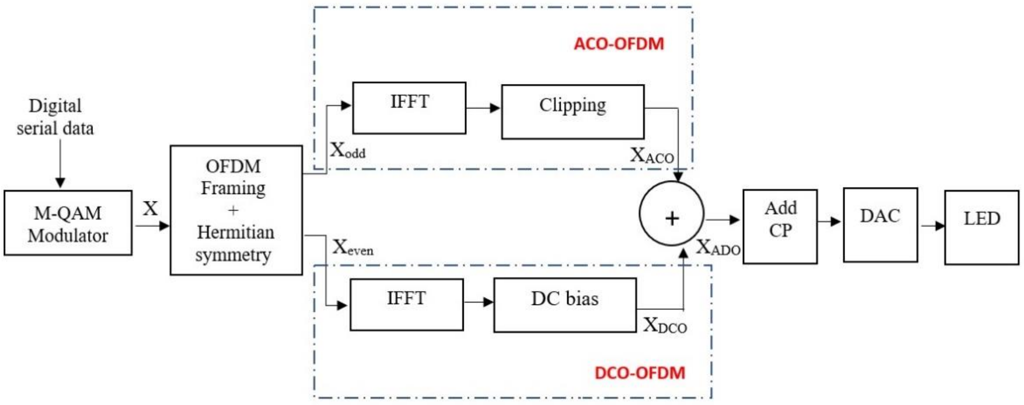

(A)

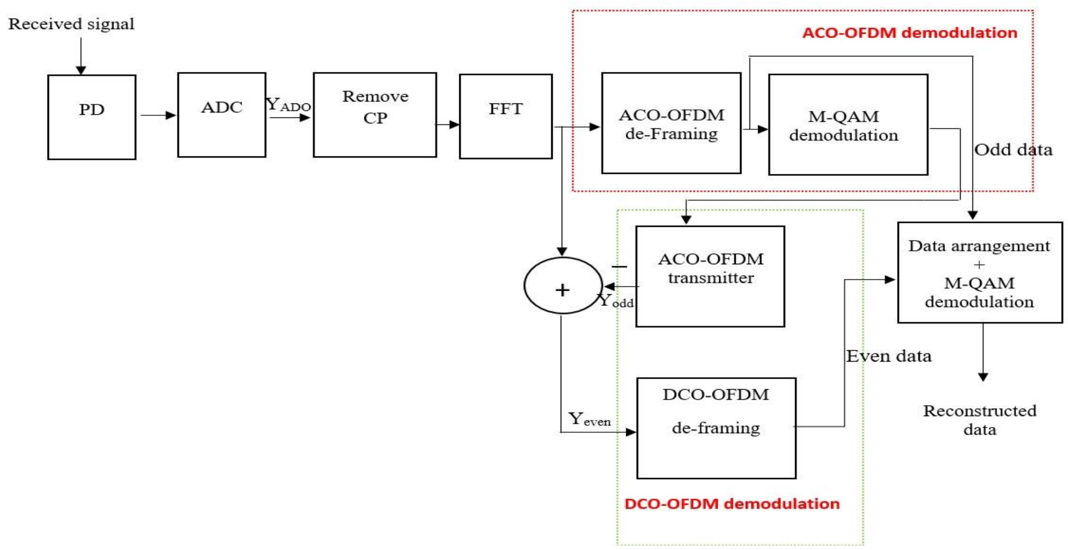

(B)

FIG. 3. ADO-OFDM BLOCK DIAGRAM (A) TRANSMITTER (B) RECEIVER [11].

Then, CP is added, and the ADO-OFDM signal is converted to analog and transformed as intensity by LED, as shown in *Fig. 3* (A). The enhanced ADO-OFDM has been proposed to overcome the complexity of the traditional ADO-OFDM receiver, as shown in *Fig. 3* (B) [11]. The ADO-OFDM receiver consists of two demodulation parts for ACO-OFDM and DCO-OFDM. The ACO-OFDM demodulation is performed directly on the odd components of the FFT process in the same scenario presented in section II.B.The DCO-OFDM demodulation is done after ACO-OFDM demodulation; the regenerated ACO-OFDM frame is subtracted from the received signal [11], [18].

Received 27/August/2021; Accepted 18/October/2021

DOI: https://doi.org/10.33103/uot.ijccce.22.2.2

D. PAPR Issue

The high value of PAPR is considered a severe drawback of OFDM systems. So, the PAPR issue is an undesired occurrence due to the IFFT process [22]. The PAPR in dB for a given OFDM signal can be evaluated as [19]:

$$PAPR = 10\,log(\frac{mAX(x(t)^2)}{E[x(t)]^2}) \tag{8}$$

where $\max(x(t)^2)$ is the peak power and $E[x(t)]^2$ is the average power. The PAPR reduction can be measured using the complementary cumulative distribution function (CCDF) [15]. The CCDF is the probability that the PAPR value reaches a certain OFDM symbol threshold and is denoted by the CCDF based on PAPR (PAPR0) [14]. The CCDF can be expressed as:

$$CCDF = Probability\;(PAPR > PAPR_0) \tag{9}$$

III. The PROPOSED MODEL

The VLC performance will be affected by high values of PAPR, which induces a nonlinear behavior and can damage the LED [19]. The most commonly extensively utilized technique for PAPR reduction is the μ- law companding [18], [19], [23]. In this paper, the proposed model for PAPR reduction involves the combination of μ-law compander and convolutional encoder. *Fig. 4* presents the proposed model for PAPR reduction with different O-OFDM systems such as DCO-OFDM, ACO-OFDM, and ADO-OFDM. The μ-law compander is added to weaken the highest peak and boost the lowest peak. The compander is placed after the O-OFDM transmitter to map the electrical domain signal before converting the signal to intensity. The mapped O-OFDM by μ- law companding can be expressed as follows [18]:

$$S = \frac{max\,(X_{O-OFDM})\cdot ln(1+\frac{\mu\cdot|X_{O-OFDM}|}{max(X_{O-OFDM})})}{ln(1+\mu)} \tag{10}$$

where $X_{O\text{-}OFDM}$ is the given O-OFDM signal and μ is the compressed parameter.

The PD detects the intensity signal at the receiver and converts it to a digital signal for processing by the de-compander and O-OFDM receiver. The μ-law de-compandor is the inverse function of compandor and is used to reconstruct the O-OFDM signal back to its original form. It can be represented as [19]:

$$S^{inv} = \frac{max\,(X_{O-OFDM})}{\mu}\cdot\left(exp^{\left(\left|\frac{S}{max(X_{O-OFDM})}\cdot ln(1+\mu)\right|\right)} - 1\right) \tag{11}$$

Received 27/August/2021; Accepted 18/October/2021
 ISSN (Print) 1811-9212 *ISSN (Online) 2617-3352*

DOI: https://doi.org/10.33103/uot.ijccce.22.2.2

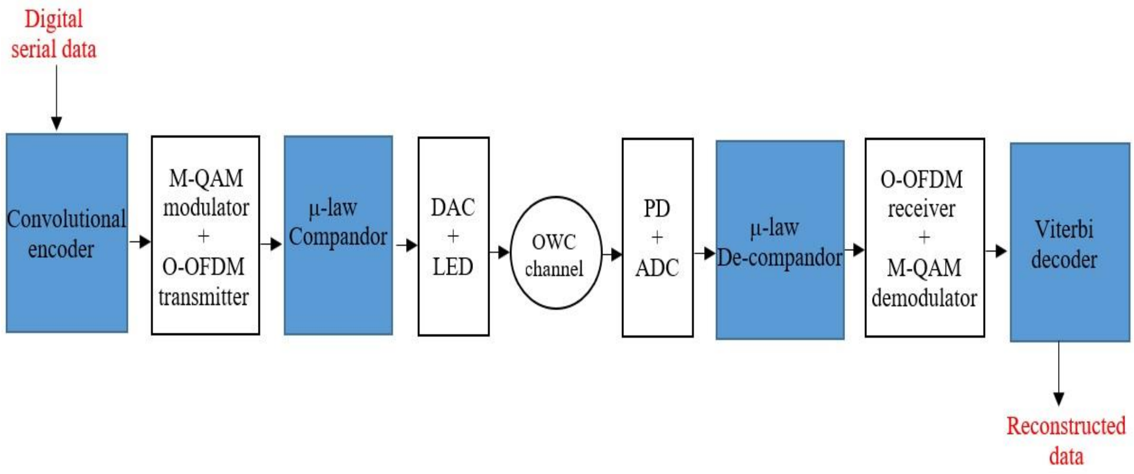

FIG. 4. PROPOSED MODEL DIAGRAM.

The utilization of μ-law compander/de-compander with the O-OFDM system can achieve a significant PAPR reduction with BER degradation in the VLC system. So, the convolutional encoder is added before the M-QAM modulator in the proposed model to improve the BER performance of VLC. However, the Viterbi decoder is used after the M-QAM demodulator. The convolutional encoder is widely utilized in digital communication. It is a type of channel coding that is easy to implement via logic gates and provides an error correction scheme [13], [24]. The convolutional code produces depending on the current state of the message input and the previous state stored in the memory cells of the encoder [24]. The increasing number of memory cells plays an essential role in increasing the complexity and error-correcting code efficiency. The general representation of the encoder can be denoted as $C_{conv}(n, k, K)$, K refers to the number of memory cells, n and k represent the number of bits for the input message and output code, respectively. *Fig. 5* presents the convolutional encoder example, referred to $C_{conv}(2, 3, 2)$ [24]. The constraint length of the encoder can be expressed as (K+1). The code is generated by convoluting the input message with the code generator sequence.

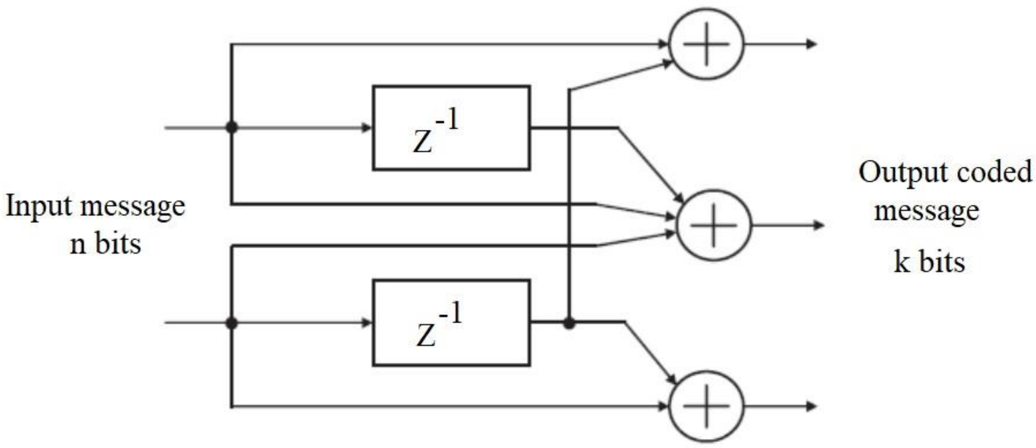

FIG. 5. CONVOLUTIONAL ENCODER EXAMPLE [24].

Received 27/August/2021; Accepted 18/October/2021
 ISSN (Print) 1811-9212 ISSN (Online) 2617-3352

DOI: https://doi.org/10.33103/uot.ijccce.22.2.2

The Viterbi decoder has been applied efficiently in the VLC system based on O-OFDM [11]. In this work, the Viterbi algorithm is used as a decoder for the convolutional encoder to correct the transmission errors caused in the VLC system due to LED nonlinearity, noise, and companding. The Viterbi algorithm accomplished maximum likelihood decoding, which improves BER. It can be used with a convolutional code trellis, which has appropriate properties to find the best path chosen by the encoder [24], [25]. The decoder deals with hard-decision or soft-decision detection methods by comparing the distance between received data and the code vector or sequence [25]. Soft-decision detection is applied in the proposed model because BER improvement is better than hard-decision. It uses different discrete quantized threshold values, which increases the detection capability of the erroneously transmitted data.

IV. SIMULATION RESULTS AND DISCUSSION

This section performs the simulation results using MatlabR2019b software for the VLC system based on different O-OFDM schemes such as ACO-OFDM, DCO-OFDM, and ADO-OFDM. The simulation is performed using PAPR for the examined O-OFDM using the parameters listed in Table I.

TABLE I. SIMULATION PARAMETERS

Parameters	**Value**
Number of O-OFDM symbols	1000
N	1024
CP	128
DC bias	[0.1V ADO-OFDM , 0.2V DCO-OFDM]
Modulation	[QAM, 256QAM]
μ	255

The CCDF performance of PAPR curves is first performed in the original form without companding for ACO-OFDM, ADO-OFDM and ADO-OFDM and then compared using the proposed model with different O-OFDM techniques to study the PAPR reduction as shown in *Fig. 6*. The CCDF of PAPR is carried out for QAM and 256 QAM modulations to illustrate the PAPR variation with modulation order. It can be seen an effective PAPR reduction has been demonstrated using the companding in the proposed model. The simulation results show that the original ACO-OFDM has a higher PAPR than the other O-OFDM. It reaches 17.5 dB at CCDF=10^{-3} for 256QAM modulation, and it is reduced to 7 dB using the proposed model. The DCO-OFDM has a lower PAPR than ACO-OFDM and is slightly smaller than ADO-OFDM. The proposed model achieves PAPR reductions of about 10 dB in ACO-OFDM, 6dB for ACO-OFDM, and 5dB in DCO-OFDM at different modulation orders.

Received 27/August/2021; Accepted 18/October/2021
 ISSN (Print) 1811-9212 ISSN (Online) 2617-3352

DOI: https://doi.org/10.33103/uot.ijccce.22.2.2

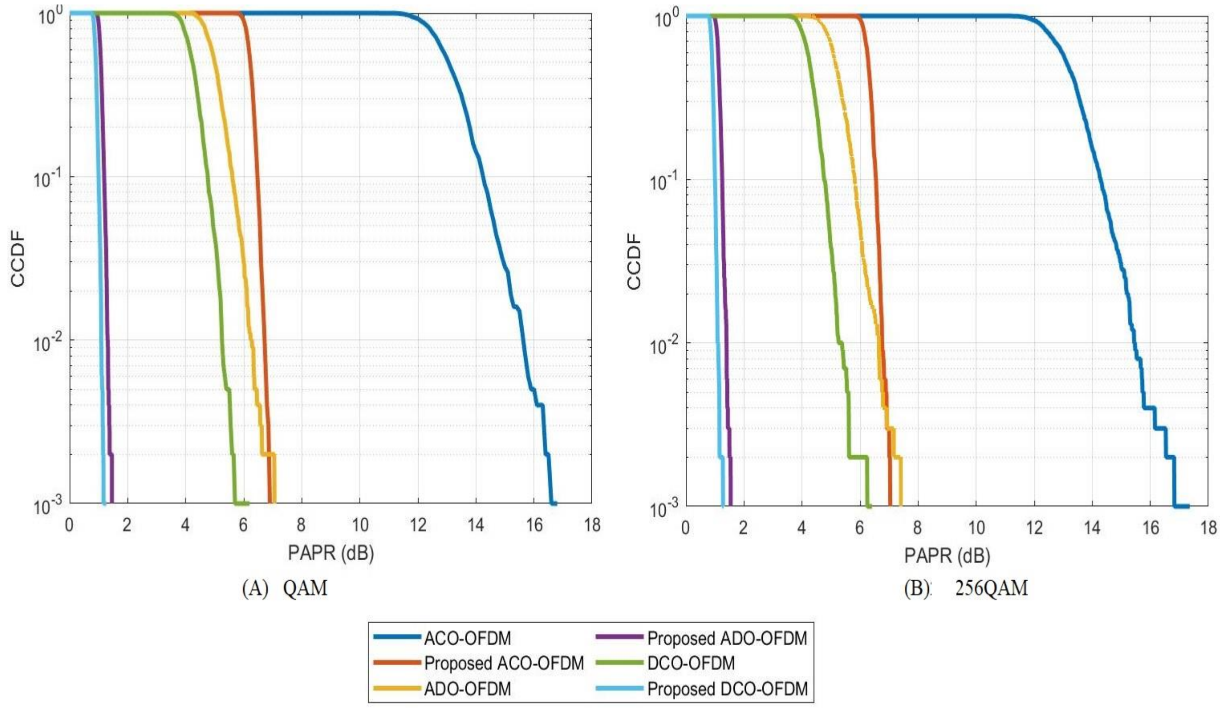

FIG. 6. CCDF PERFORMANCE FOR DIFFERENT O-OFDM-BASED VLC.

Another essential performance parameter for VLC communication systems is BER. The μ-law compandor is a good technique for PAPR reduction but at the expense of BER. Three encoder schemes are used in this work to study the BER and compare them to get the best improvement. The first is a proposed convolutional encoder with parameters: $C_{conv}(2, 3, 9)$, constraint length of the lower path 5, and 6 for the upper. The code generators in octal numbering for the upper memory cells of the encoder are $(57\ 24\ 0)_8$ and $(0\ 35\ 31)_8$ for the lower taps. The second type is the convolutional encoder proposed in [13], referred to as $C_{conv}(2, 3, 7)$. However, the last encoder examined is a Hamming encoder/decoder proposed in [11] used with VLC based O-OFDM with n=4 and k=7. The considered encoders do not affect the PAPR results, but they have a basic rule to reduce BER. As a result, the proposed PAPR reduction model has improved both BER and PAPR in VLC system-based O-OFDM.

The BER performance for ACO-OFDM, ADO-OFDM, and DCO-OFDM are illustrated from *Fig. 7-9* under different cases. The BER is evaluated for the investigated O-OFDM techniques in the original scenario (without companding) and compared using the proposed model. The BER is computed for the proposed model with varying encoder schemes.

Fig. 7 results show that the BER performance is better than ADO-OFDM and DCO-OFDM due to simplicity in design that relies only on the odd subcarriers at the expense of spectral efficiency and does not requiring DC bias. In ACO-OFDM, BER can be increased from 0.0314 to 1.95×10^{-6} at SNR= 14dB for QAM and from 0.065 to 6.5×10^{-4} at SNR=22dB for 256QAM. It has been shown that the convolutional encoder improves BER upon higher-order modulation to the original state (without companding). In VLC, the ADO-OFDM approach is an enhanced O-OFDM technique, with performance results shown in *Fig. 8*. The BER of QAM at SNR= 28 dB is improved from 0.4 to 0.004 with Cconv(2, 3, 7) and gets even better up to 10^{-4} with Cconv(2, 3, 9). However, for 256QAM, the proposed model becomes better than in the original case it raised from 10^{-3} to 1.5×10-5 at SNR=38 dB.

Received 27/August/2021; Accepted 18/October/2021
 ISSN (Print) 1811-9212 *ISSN (Online) 2617-3352*

DOI: https://doi.org/10.33103/uot.ijccce.22.2.2

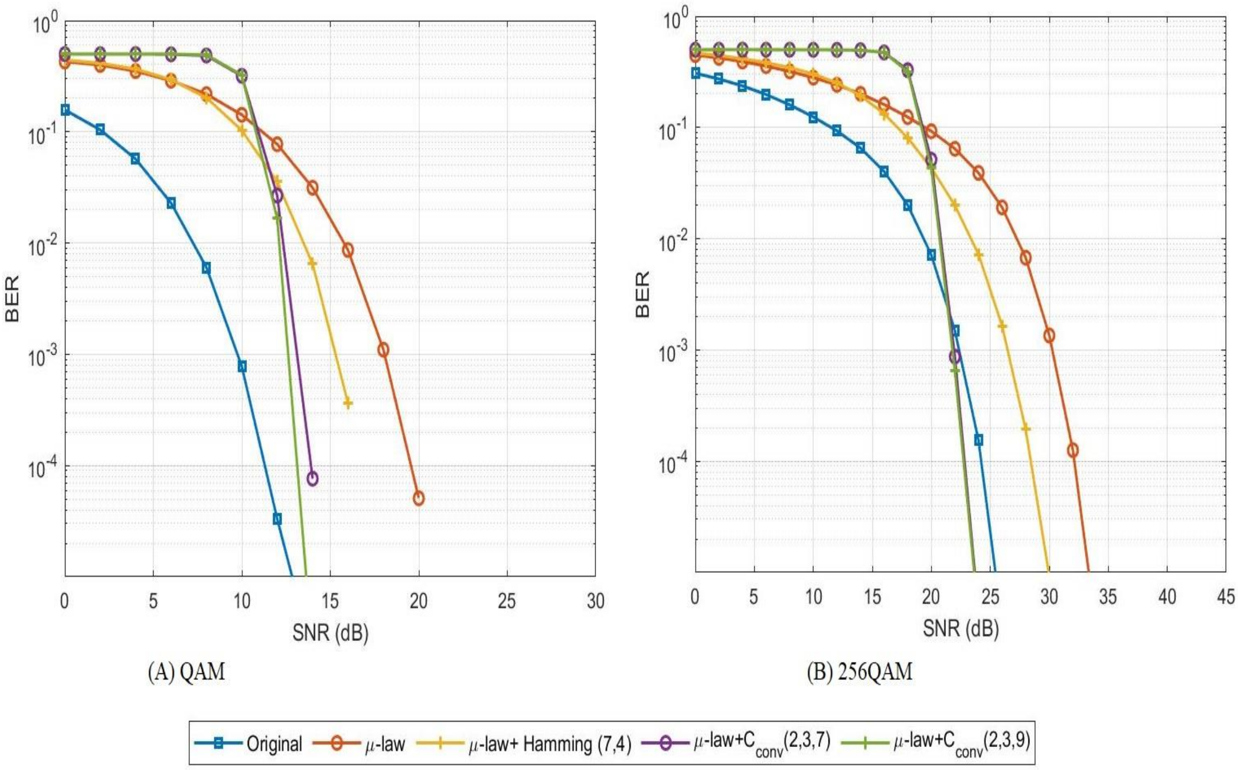

FIG. 7. BER PERFORMANCE FOR ACO-OFDM UNDER DIFFERENT SCHEMES.

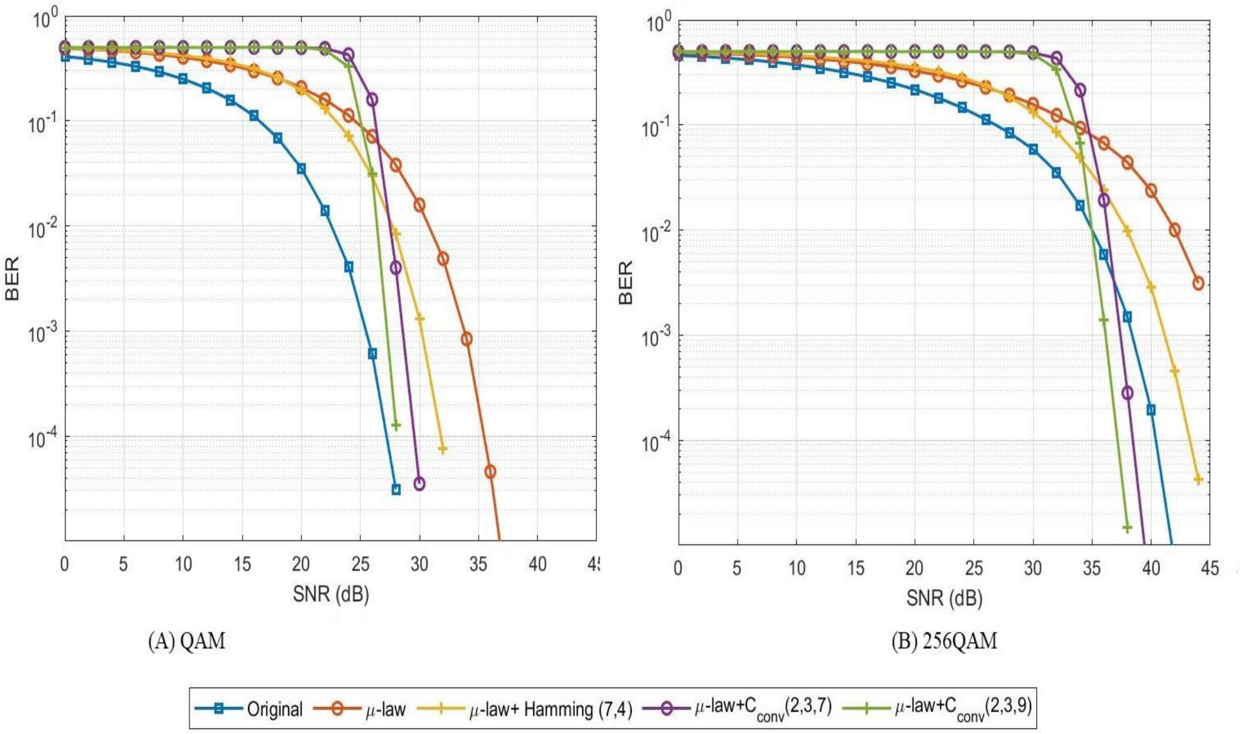

FIG. 8. BER PERFORMANCE FOR ADO-OFDM UNDER DIFFERENT SCHEMES.

Received 27/August/2021; Accepted 18/October/2021

ISSN (Print) 1811-9212 *ISSN (Online) 2617-3352*

DOI: https://doi.org/10.33103/uot.ijccce.22.2.2

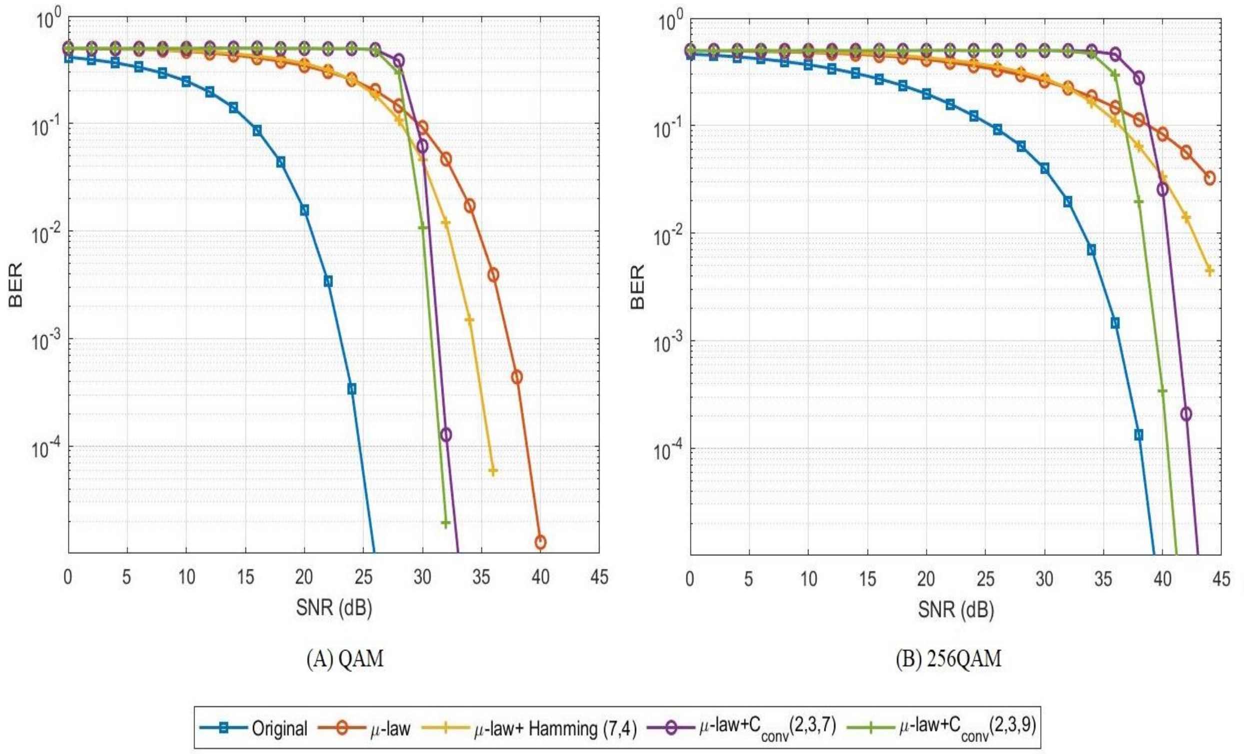

FIG. 9. BER PERFORMANCE FOR DCO-OFDM UNDER DIFFERENT SCHEMES.

The convolutional encoder achieves good BER results and outperforms the original ADO-OFDM (without compounding) performance in 256QAM. Although ADO-OFDM is more complex than DCO-OFDM, the convolutional encoder with soft coding makes ADO-OFDM performance better than DCO-OFDM. In *Fig. 9*, DCO-OFDM has bad BER performance with μ-law companding (without coding) and about 15dB BER degradation at BER=10^{-4} for QAM. The BER can be improved from 0.017 to 10^{-3} in DCO-OFDM for SNR=32 dB using QAM modulation, while for the case of 256QAM in the same considerations, BER is not changed. While the Cconv(2, 3, 9) can improve BER from 0.08 to 10^{-4} at SNR=42 dB for 256QAM.

The results exhibit that uncoded μ-law compander reduce PAPR while degrades the BER for all O-OFDM techniques and under different modulations. However, the increasing modulation order leads to the increment of BER and PAPR. It can be seen that Hamming encoder/decoder is effective for simple errors correction of VLC based O-OFDM systems.

In contrast, the convolutional encoder with Viterbi algorithm-based soft-decision can achieve better performance. Also, the number of memory cells in the convolutional encoder can powerfully improved BER. Table II summarizes the signal-to-noise ratio (SNR) comparisons between ACO-OFDM, ADO-OFDM, and DCO-OFDM for different cases at BER=10^{-3} clarifying the improvement.

Received 27/August/2021; Accepted 18/October/2021
 ISSN (Print) 1811-9212 *ISSN (Online) 2617-3352*

DOI: https://doi.org/10.33103/uot.ijccce.22.2.2

TABLE II. PERFORMANCE COMPARISON BETWEEN DIFFERENT O-OFDM TECHNIQUES AT BER=10^{-3}

O-OFDM type	Signal-to-Noise Values (dB)				
	Original	**μ-law**	**μ-law with Hamming (7,4)**	**μ-law with Cconv(2, 3, 7)**	**μ-law with Cconv(2, 3, 9)**
ACO-OFDM (QAM)	9.5	18	15.5	14	13
ADO-OFDM (QAM)	25	33.5	30	28.5	27
DCO-OFDM (QAM)	23	37.5	34	31.5	31
ACO-OFDM (256QAM)	23	30.5	27	22	22
ADO-OFDM (256QAM)	38	46	41	37.5	36
DCO-OFDM (256QAM)	36	50	41	37.5	36

Table III presents the BER and PAPR comparison between the proposed model using μ-law with Cconv(2, 3, 9) and different PAPR reduction methods that include uncoded μ-law compander, clipping method and combination PAPR reduction approach based μ-law compander and clipping. The PAPR reduction method based μ-law and clipping were illustrated in [18]. The PAPR and SNR gain is evaluated for 10^{-3} CCDF and BER. Although the μ-law and clipping approach achieve the best value for PAPR reduction, it suffers from lousy BER performance, especially for higher-order modulation due to interference through clipping. However, the proposed model makes a tradeoff between the BER and PAPR.

TABLE III. PAPR & BER COMPARISON FOR DIFFERENT PAPR REDUCTION METHODS

O-OFDM type	**Original**		**Uncoded μ-law**		**μ-law with clipping** [18]		**Clipping** [18]		**μ-law with Cconv(2, 3, 9)**	
	PAPR (dB)	**SNR (dB)**	**PAPR (dB)**	**SNR (dB)**	**PAPR (dB)**	**SNR (dB)**	**PAPR (dB)**	**SNR (dB)**	**PAPR (dB)**	**SNR (dB)**
ACO-OFDM (QAM)	16.9	9.5	7	18	5.85	19	15	10	7	13
ADO-OFDM (QAM)	7.07	25	1.46	33.5	1	34	4.64	26	1.46	27
DCO-OFDM (QAM)	6.25	23	1.27	37.5	0.622	39	3.47	24	1.27	31
ACO-OFDM (256QAM)	17.37	23	7.05	30.5	5.93	45	12.33	32	7.05	22
ADO-OFDM (256QAM)	7.41	38	1.54	46	1	60	4.9	45	1.54	36
DCO-OFDM (256QAM)	6.42	36	1.31	50	0.73	54	4.33	36	1.31	36

Received 27/August/2021; Accepted 18/October/2021

DOI: https://doi.org/10.33103/uot.ijccce.22.2.2

V. CONCLUSIONS

The PAPR is a prominent issue accompanying the O-OFDM system, which degrades the performance of the VLC and introduces nonlinearity. The PAPR and BER of the ACO-OFDM, ADO-OFDM, and DCO-OFDM have been investigated in this paper. The use of μ -law companding/de-companding in the proposed model has been observed to effectively reduces PAPR for different O-OFDM techniques. Simulation results show a PAPR decrease of about 10 dB in ACO-OFDM. However, PAPR is compressed by a significant amount for DCO-OFDM and ADO-OFDM and can reach PAPR values less than 1.5 dB. Even though companding techniques are required to compensate PAPR, it degrades BER performance, so a convolutional encoder with Viterbi decoder-based soft-decision has been used in the proposed model for BER improvement. The general structure of the encoder can be customized to have many memory levels to enforce the performance, but the complexity rises as well. Several simulations have been performed using $C_{conv}(2, 3, 7)$, $C_{conv}(2, 3, 9)$ convolutional encoders, and also Hamming coder/decoder (7,4). The BER graphs have shown that the proposed model-based $C_{conv}(2, 3, 9)$ satisfies the best BER improvement in VLC systems. Additionally, the proposed model has been compared with other PAPR reduction methods such as the uncoded μ-law, clipping, and combing approach of μ-law with clipping. The results have shown the excellent achievement for the proposed model that tradeoff between PAPR and BER for different O-OFDM techniques.

REFERENCES

[1] N. Sharan and S. K. Ghorai, "Hybrid scheme of precoder with μ-law compander for PAPR reduction and nonlinearity improvement in ADO-OFDM system," *Int. J. Commun. Syst.*, vol. n/a, no. n/a, p. e4961, Aug. 2021, doi: https://doi.org/10.1002/dac.4961.

[2] S. Yahia, Y. Meraihi, A. Ramdane-Cherif, A. B. Gabis, D. Acheli, and H. Guan, "A survey of channel modeling techniques for Visible Light Communications," *J. Netw. Comput. Appl.*, vol. 194, no. December 2020, p. 103206, 2021, doi: 10.1016/j.jnca.2021.103206.

[3] H. F. Abdalla, E. S. Hassan, M. I. Dessouky, and A. S. Elsafrawey, "Three-Layer PAPR Reduction Technique for FBMC Based VLC Systems," *IEEE Access*, vol. 9, pp. 102908–102916, 2021, doi: 10.1109/ACCESS.2021.3098776.

[4] G. Miriyala and V. V. Mani, "A nonlinear modelled low-complex ADO-OFDM for Visible light communication systems," *Optik (Stuttg).*, vol. 246, no. July, p. 167831, 2021, doi: 10.1016/j.ijleo.2021.167831.

[5] S. Ariyanti and M. Suryanegara, "Visible light communication (VLC) for 6G technology: The potency and research challenges," *Proc. World Conf. Smart Trends Syst. Secur. Sustain. WS4 2020*, no. Vlc, pp. 490–493, 2020, doi: 10.1109/WorldS450073.2020.9210383.

[6] S. U. Rehman, S. Ullah, P. H. J. Chong, S. Yongchareon, and D. Komosny, "Visible light communication: A system perspective—Overview and challenges," *Sensors (Switzerland)*, vol. 19, no. 5, pp. 1–22, 2019, doi: 10.3390/s19051153.

[7] A. Singh, A. Jain, and P. Vyavahare, "A study of peak to average power ratio for different companding techniques in VLC-OFDM system," *2016 Int. Conf. Adv. Comput. Commun. Informatics, ICACCI 2016*, pp. 2390–2393, 2016, doi: 10.1109/ICACCI.2016.7732413.

[8] S. D. Dissanayake and J. Armstrong, "Comparison of ACO-OFDM, DCO-OFDM and ADO-OFDM in IM/DD Systems," *J. Light. Technol.*, vol. 31, no. 7, pp. 1063–1072, 2013, doi: 10.1109/JLT.2013.2241731.

[9] A. A. Abdulkafi, M. Y. Alias, and Y. S. Hussein, "Performance analysis of DCO-OFDM in VLC system," *2015 IEEE 12th Malaysia Int. Conf. Commun. MICC 2015*, vol. 1, no. Micc, pp. 163–168, 2016, doi: 10.1109/MICC.2015.7725427.

[10] U. Choudhary and V. Janyani, "Bandwidth efficient frame structures for flip OFDM with phase conjugated sub carriers and LDPC encoding," *Optik (Stuttg).*, vol. 204, no. January, p. 164175, 2020, doi: 10.1016/j.ijleo.2020.164175.

[11] S. M. Hameed, S. M. Abdulsatar, and A. A. Sabri, "Performance enhancement for visible light communication based ADO-OFDM," *Opt. Quantum Electron.*, vol. 53, no. 6, p. 339, 2021, doi: 10.1007/s11082-021-02965-1.

[12] H. Qian, S. J. Yao, S. Z. Cai, and T. Zhou, "Adaptive postdistortion for nonlinear LEDs in visible light communications," *IEEE Photonics J.*, vol. 6, no. 4, pp. 1–8, 2014, doi: 10.1109/JPHOT.2014.2331242.

Received 27/August/2021; Accepted 18/October/2021

DOI: https://doi.org/10.33103/uot.ijccce.22.2.2

[13] S. Hameed, S. Abdulsatar, and A. Sabri, "BER Comparison and Enhancement of Different Optical OFDM for VLC," *Int. J. Intell. Eng. Syst.*, vol. 14, no. 4, pp. 326–336, Aug. 2021, doi: 10.22266/ijies2021.0831.29.

[14] A. A. Abdulkafi, M. Y. Alias, Y. S. Hussein, N. Omar, and M. K. Bin Salleh, "A hybrid papr reduction scheme for optical wireless OFDM communication systems," *KSII Trans. Internet Inf. Syst.*, vol. 12, no. 3, pp. 1136–1151, 2018, doi: 10.3837/tiis.2018.03.009.

[15] A. A. Abdulkafi, M. Y. Alias, Y. S. Hussein, N. Omar, and M. K. Bin Salleh, "PAPR reduction of DC biased optical OFDM using combined clipping and PTS techniques," *2017 IEEE 13th Malaysia Int. Conf. Commun. MICC 2017*, vol. 2017-Novem, no. Micc, pp. 207–212, 2018, doi: 10.1109/MICC.2017.8311760.

[16] H. Lu, Y. Hong, L.-K. Chen, and J. Wang, "On the study of the relation between linear/nonlinear PAPR reduction and transmission performance for OFDM-based VLC systems," *Opt. Express*, vol. 26, no. 11, p. 13891, 2018, doi: 10.1364/oe.26.013891.

[17] I. A. Shaheen, A. Zekry, F. Newagy, and R. Ibrahim, "Performance evaluation of PAPR reduction in FBMC system using nonlinear companding transform," *ICT Express*, vol. 5, no. 1, pp. 41–46, 2019, doi: 10.1016/j.icte.2018.01.017.

[18] O. Singh, R. Paulus, and R. Srivastava, "PAPR reduction scheme for optical OFDM techniques," *J. Opt. Commun.*, no. November, Nov. 2020, doi: 10.1515/joc-2020-0206.

[19] N. Sharan and S. K. Ghorai, "PAPR reduction and non-linearity alleviation using hybrid of precoding and companding in a visible light communication (VLC) system," *Opt. Quantum Electron.*, vol. 52, no. 6, 2020, doi: 10.1007/s11082-020-02426-1.

[20] P. P. Jativa, C. A. Azurdia-Meza, M. R. Canizares, D. Zabala-Blanco, and S. Montejo-Sanchez, "Performance Analysis of OFDM-Based VLC Schemes in NLOS Channels," *2020 South Am. Colloq. Visible Light Commun. SACVC 2020 - Proc.*, 2020, doi: 10.1109/SACVLC50805.2020.9129862.

[21] S. E. D. N. Mohamed, A. E. N. A. Mohamed, F. E. A. El-Samie, and A. N. Z. Rashed, "Performance enhancement of IM/DD optical wireless systems," *Photonic Netw. Commun.*, vol. 36, no. 1, pp. 114–127, 2018, doi: 10.1007/s11107-018-0761-0.

[22] M. A. Hussein, A. H. Ali, and A. K. Nahar, "Hybrid Model for PAPR Minimization in OFDM System," *Iraqi J. Comput. Commun. Control Syst. Eng.*, pp. 16–30, Feb. 2021, doi: 10.33103/uot.ijccce.21.1.2.

[23] Y. Yang, Z. Zeng, S. Feng, and C. Guo, "A Simple OFDM Scheme for VLC Systems Based on μ-Law Mapping," *IEEE Photonics Technol. Lett.*, vol. 28, no. 6, pp. 641–644, 2016, doi: 10.1109/LPT.2015.2503481.

[24] J. Castiñeira Moreira and P. G. Farrell, *Essentials of Error-Control Coding*. 2006.

[25] T. Adiono, Y. Aska, S. Fuada, and A. A. Purwita, "Design of an OFDM System for VLC with a Viterbi Decoder," *IEIE Trans. Smart Process. Comput.*, vol. 6, no. 6, pp. 455–465, Dec. 2017, doi: 10.5573/IEIESPC.2017.6.6.455.

Received 27/August/2021; Accepted 18/October/2021